Award Number: W81XWH-20-1-0429

TITLE: Development of 5D3 mAb and USPIO-Based Theranostics for Image-Guided Prostate Cancer Therapy

PRINCIPAL INVESTIGATOR: Sudath Hapuarachchige, Ph.D.

CONTRACTING ORGANIZATION: Johns Hopkins University, Baltimore, MD

REPORT DATE: July 2022

TYPE OF REPORT: Annual Report

PREPARED FOR: U.S. Army Medical Research and Development Command
Fort Detrick, Maryland 21702-5012

REPORT DOCUMENTATION PAGE

Form Approved
OMB No. 0704-0188

PLEASE DO NOT RETURN YOUR FORM TO THE ABOVE ADDRESS.

1. REPORT DATE *(DD-MM-YYYY)*	2. REPORT TYPE	3. DATES COVERED *(From - To)*
July 2022	Annual Report	15Jun2021-14Jun2022

4. TITLE AND SUBTITLE

Development of 5D3 mAb and USPIO-Based Theranostics for Image-Guided Prostate Cancer Therapy

5a. CONTRACT NUMBER

W81XWH-20-1-0429

5b. GRANT NUMBER

5c. PROGRAM ELEMENT NUMBER

6. AUTHOR(S)

Sudath Hapuarachchige, Ph.D.

E-mail: shapuar1@jh.edu

5d. PROJECT NUMBER

5e. TASK NUMBER

5f. WORK UNIT NUMBER

7. PERFORMING ORGANIZATION NAME(S) AND ADDRESS(ES)

Johns Hopkins University, 3400 N Charles St., Baltimore, MD 21218-2608

8. PERFORMING ORGANIZATION REPORT NUMBER

9. SPONSORING/MONITORING AGENCY NAME(S) AND ADDRESS(ES)

U.S. Army Medical Research and Development Command
Fort Detrick, Maryland 21702-5012

10. SPONSOR/MONITOR'S ACRONYM(S)

11. SPONSOR/MONITOR'S REPORT NUMBER(S)

12. DISTRIBUTION/AVAILABILITY STATEMENT

Approved for Public Release; Distribution Unlimited

13. SUPPLEMENTARY NOTES

14. ABSTRACT

Prostate cancer (PC) is the most common cancer in men and associated with the second highest cancer related mortality. Therefore, new treatment strategies including novel drugs and drug delivery systems are urgently needed for PC therapy. Prostate-specific membrane antigen (PSMA) is overexpressed in almost all PC. PSMA is used as a biomarker for targeted drug delivery and diagnostic imaging of PC. 5D3 mAb is a novel antibody with better circulation half-time, higher binding affinity with PSMA, and fast internalization kinetics compared to commercially available anti-PSMA mAbs. In this study, we have been using ultra-small superparamagnetic iron oxide (USPIO) nanoparticles as the drug delivery platform to delivery DM1. During last two years, we have successfully developed a USPIO-5D3-DM1 conjugates and studied them in preclinical mouse models. Novel acidic linker (AL) was developed for the conjugation of DM1 with USPIO. We have developed a HPLC method and AL linker was tested for the controlled release of drugs in a dextran platform. In the third year, we will conjugate DM1 with USPIO-5D3 system using AL linker, labeled them with 89Zr to image by PET-MRI. Therapeutic and toxicological studies will be conducted in human PC xenograft mouse models.

15. SUBJECT TERMS

None listed.

16. SECURITY CLASSIFICATION OF:			17. LIMITATION OF ABSTRACT	18. NUMBER OF PAGES	19a. NAME OF RESPONSIBLE PERSON
a. REPORT	b. ABSTRACT	c. THIS PAGE			USAMRDC
U	U	U	UU	21	19b. TELEPHONE NUMBER *(Include area code)*

ANNUAL REPORT - YEAR 2

TABLE OF CONTENT

1. INTRODUCTION

Prostate cancer (PC) is the most common cancer type in men. Almost all PCs eventually become castrate-resistant prostate cancer (CRPC) and progress to metastatic cancer (mCRPC) that is an uncurable disease. Conventional drugs, such as docetaxel and cabazitaxel show lack efficacy in mCRPC. Therefore, new treatment strategies including novel drugs and drug delivery systems are urgently needed for PC therapy. Prostate-specific membrane antigen (PSMA) is overexpressed in almost all prostate cancers (PC) and used as a biomarker for targeted drug delivery and diagnostic imaging. 5D3 is a novel anti-PSMA monoclonal antibody (mAb). It has a better circulation half-time, higher binding affinity with PSMA, and fast internalization kinetics compared to commercially available anti-PSMA mAbs. In this study, we have been using ultra-small superparamagnetic iron oxide (USPIO) nanoparticles as the drug delivery platform to delivery potent anti-tubulin agent, DM1. USPIOs are biocompatible and have a high loading capacity for cargo molecules. When USPIOs are conjugated with 5D3 mAb the drug can be delivered directly to the PSMA(+) prostate cancer. Since USPIO is an MRI contrast agent, the drug delivery and tumor uptake can be detected by MRI. USPIO can also be labeled with fluorophores and/or PET tracers and tracked *in vivo* by optical and PET imaging, respectively. We have proposed a new pH-sensitive acidic linker (AL) to conjugate the DM1 drug with USPIO. Proposed AL linker is stable at neutral to high pH range (pH $\geq$7.0) and cleavable in acidic pH conditions (pH 4.5-5.5). Therefore, DM1 conjugated via AL linker will not dissociate from USPIO in the circulation and will be effectively released after internalization followed by the accumulation in late endosomes and lysosomes at low pH.

2. KEYWORDS: Prostate cancer, Prostate-specific membrane antigen, antibody, ultra-small superparamagnetic iron oxide nanoparticles, image-guided targeted therapy, theranostics, preclinical imaging**.**

3. ACCOMPLISHMENTS

During the second year of the project, we designed, synthesized, and characterized the DM1-AL and study the release of drugs. The synthesis of this novel and acid sensitive AL linker was critical because it should provide stability and controlled release of the conjugated drugs. We have carefully designed and optimized the synthetic route and developed the DM1-amine intermediate followed by the DM1-AL product. These two compounds were characterized by ^{1}H NMR and the molecular weights were determined by the MALDI-TOF. The drug release was evaluated using the dextran platform. We have developed a method for the determination of trace DM1 and its residues using HPLC. The concentrations of the released DM1 were determined by the HPLC protocol in low and high pH conditions at 5 and 24 h time points. We have successfully accomplished the development and validation of the drug/DM1 conjugation strategy.

We have submitted two conference abstracts, (a) annual meeting of ISMRM 2022, and (b) annual meeting of WMIC 2022 based on the results and discoveries of this project.

We have collaborated and supported Dmitri Artemov's group for the conjugation techniques and characterization of USPIO nanoparticles. Their results and discoveries were recently published in the journal, *ACS Applied Nano Materials* (https://pubs.acs.org/doi/10.1021/acsanm.2c01835). Our contribution and this DOD grant were acknowledged in the "Contribution" and "Funding" sections.

What were the major goals of the project?
Specific Aims of the proposal are:

Specific Aim 1: To develop and optimize USPIO(5D3)(DM1) nano-theranostics and evaluate them *in vitro*. (1-9 months, 100% completion)
Major Task 1: Synthesis and characterization of USPIO(5D3)(DM1)(Fluor)
Major Task 2: Validation of USPIO(5D3)(DM1)(Fluor) for binding affinity, internalization and *in vitro* therapeutic efficacy in PSMA(±) PC cells.

Specific Aim 2: To determine the pharmacokinetics and biodistribution of USPIO(5D3)(DM1) nano-theranostics in PSMA(±) mouse models of human PC. (10-24 months, 75% completion)
Major Task 1: Study the pharmacokinetics of USPIO(5D3)(DM1)(^{89}Zr-DFO) by γ-counting.
Major Task 2. Study of the biodistribution of USPIO(5D3)(DM1)(^{89}Zr-DFO) by *in vivo* by PET-MRI and *ex vivo* by γ-counting and ICP-MS.

Specific Aim 3: To determine the toxicology, tumor uptake, and treatment response of USPIO(5D3)(DM1) nano-theranostics in PSMA(±) mouse models of human PC.
Major Task 1: Determination of the toxicology of USPIO(5D3)(DM1) *in vivo* in mouse models of human PC.
Major Task 2: Investigation of the tumor uptake of USPIO(5D3)(DM1) by MRI and treatment response by ^{18}F-DCFPyL PET in mouse models of human PC.

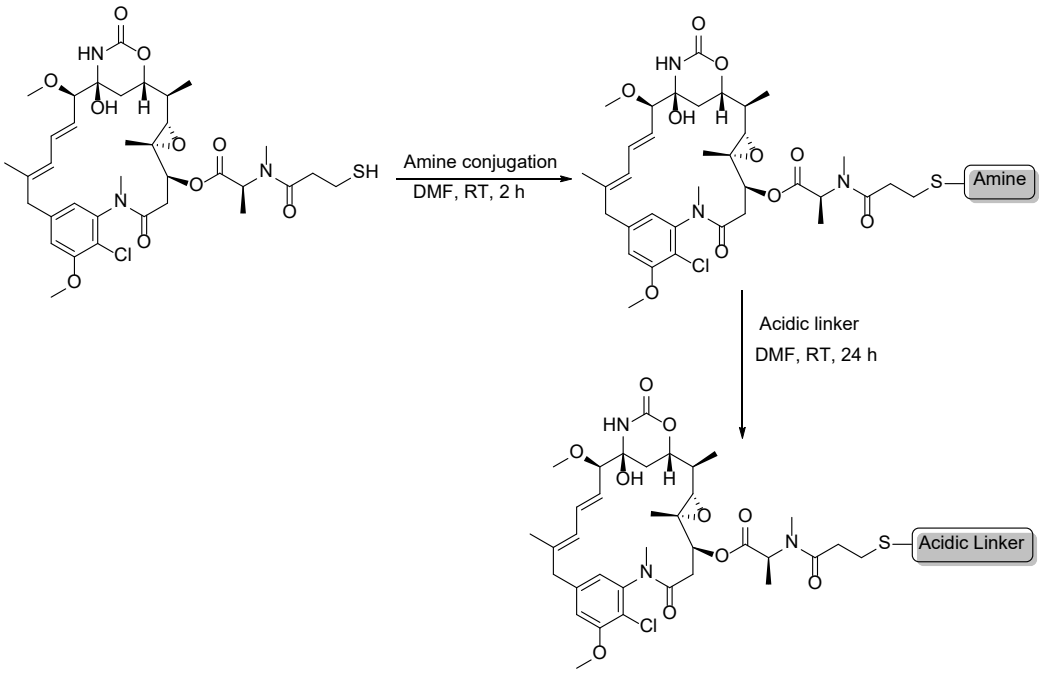

Scheme 1. Synthesis of DM1-AL. (i) DM1 was reacted with amine compound DM1-amine. (ii) The resultant product, DM1-amine was then treated with acidic linker to obtain DM1-AL.

What was accomplished under these goals?

(i) Synthesis of DM1-AL: We have successfully synthesized mertansine-acidic linker (DM1-AL, **Scheme 1**) and characterized by ^{1}H NMR and HPLC-MS (**Figure 1**). In the synthesis of DM1-AL, first, DM1 was reacted with amine functional group to produce DM1-amine. The resultant product, DM1-amine was then treated with the acidic linker. The resultant, DM1-AL (**Figure 2**) was obtained as a white solid. The intermediate DM1-amine and the final product DM1-AL were purified by a column chromatography and characterized by MALDI-TOF spectrometry and ^{1}H NMR.

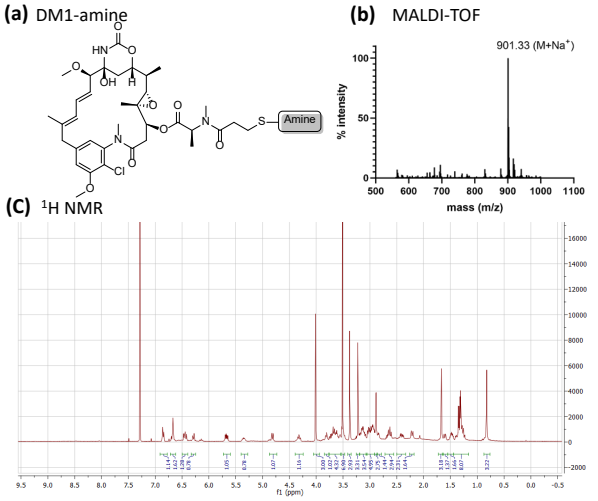

Figure 1. Characterization of DM1-amine. (a) Structure of DM1-amine, (b) MALDI-TOF spectrum, and (c) ^{1}H NMR spectrum.

(ii) Development of HPLC method: We have developed a HPLC protocol to determine trace concentrations of DM1 in the extraction samples. We used a Waters dual pump HPLC system with C18 reverse phase analytical column using a 70% acetonitrile/water/0.1% TFA solvent mixture as the mobile phase. For the calibration curve, standard series of DM1 samples (5-250 ng/mL) was injected (10 uL) and run using the 70% acetonitrile/water/0.1% TFA solvent mixture. Areas under the curve were recorded and plotted against the concentrations (**Figure 3a**) with the lower limit of detection (LLOD) of 5 ng/ml.

(iii) Drug-release study: We conducted a DM1-AL acid drug release experiment using a dextran platform. Here, dextran (2 MDa) was treated with 10% of DM1-AL in PBS (pH 7.5). The mixture was stirred for 6 h at room temperature. The resultant product, dextran-AL-DM1, was purified by centrifugal ultrafiltration using 30 kDa molecular weight cut-off (MWCO) filter units. Two aliquots of dextran-AL-DM1 were incubated in PBS at pH adjusted to 5.5 and 7.5. The aliquots were stirred at room temperature and samples were taken at 5- and 24-h time-points. The free drug released from the dextran platform was isolated by filtration using 30 kDa MWCO filter units. The concentration of DM1 in filtrates was determined by the HPLC method, as described above.
The results exhibited the highest release of drugs at pH 5.5 after 24 h compared to all other conditions. In basic pH conditions, the AL bond is stable, and the drug is not released from the dextran platform.

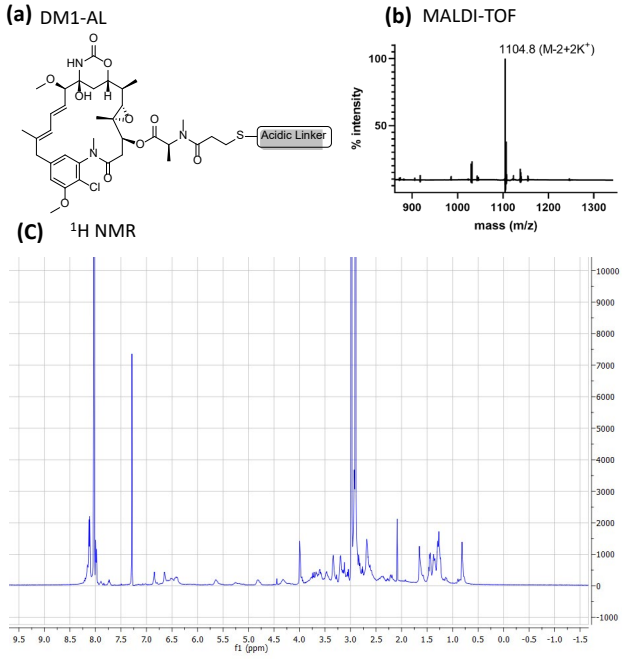

Figure 2. Characterization of DM1-AL. (a) Structure of DM1-AL, (b) MALDI-TOF spectrum, and (c) ^{1}H NMR spectrum.

However, in acidic pH 5.5, the AL bond is hydrolyzed, and drug is completely released within 24 h. Interestingly, the drug release at pH 5.5 is still below 20% after 5 h, suggesting the relative stability of the AL bond and controlled release with time (**Figure 3b**). The mechanism of drug release is shown in **Scheme 2**. In spite of acidic tumor microenvironments the controlled release provides ADC a sufficient time to internalize into targeted PSMA(+) prostate cancer cells for improved therapeutic index. The drug is not released in the circulatory system and vital organs such as kidney and liver at neutral and basic pH conditions.

Here, the pH-dependent releasing concept was proved for the dextran platform, as a model for DM1 conjugation with 5D3. After releasing the drug, the linker "tether" is still attached to the drug molecule; however, our previous experiments proved that the substitution on the DM1 thiol group does not significantly affect therapeutic activity. Our proposed drug delivery strategy will enhance the target-specific release, providing high therapeutic efficacy of ADCs.

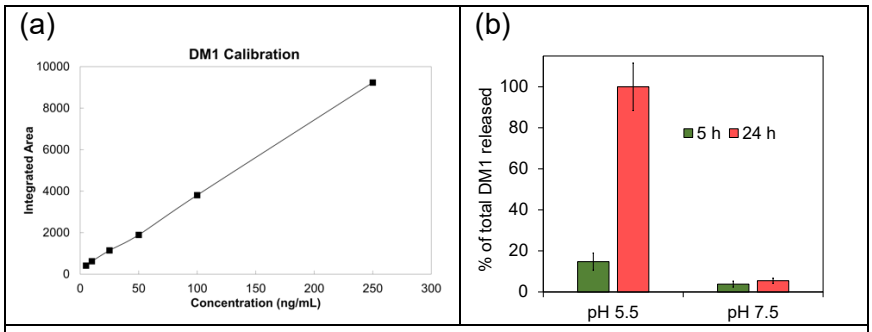

Figure 3. Determination of DM1 concentration. (a) Calibration curve for HPLC method. (b) Percentage of total DM1 released at pH 5.5 and 7.5.

What opportunities for training and professional development has the project provided?

We participated virtual annual meeting of ISMRM and attended online presentation to broaden our knowledge on current research work relevant to this project. One graduate student (collaboration) and an undergraduate student (volunteer) were partially worked in this project. We provided training for conjugation chemistry, characterization of antibody and USPIO. They will continue the training program in the Fall 2022.

How were the results disseminated to communities of interest?

An abstract was submitted for the annual meeting of International Society for Magnetic Resonance in Medicine (ISMRM) and a presentation (virtual) was given at held in London, UK in May 2022. An abstract was submitted for a presentation at the annual meeting of World Molecular Imaging Congress (WMIC) in Miami, FL, USA in September 2022. The chemistry and bioconjugation techniques used in this project were utilized in the collaborative studies and the results were published in the journal, *ACS Applied Nano Materials*.

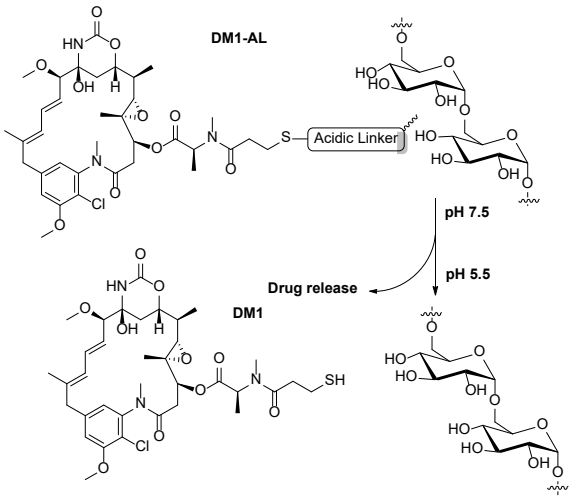

Scheme 2. Release of DM1 drugs from dextran at low pH condition.

What do you plan to do during the next reporting period to accomplish the goals?

During the first year we conjugated USPIO with 5D3 and labeled with fluorophores. This system was optimized for optical and MRI imaging. In the second year we have developed the AL system, conjugated with DM1, and evaluated the drug

release from dextran platform by HPLC techniques. During the next reporting period, we will integrate USPIO-5D3 targeted drug delivery system with DM1 through the AL. The resultant, USPIO-5D3-AL-DM1 will be further labeled with ^{89}Zr. The completed and radiolabeled drug delivery system will be evaluation in PC xenograft mouse models using PET-MRI imaging system. Therapeutic efficacy, biodistribution, pharmacokinetics will be studied *in vivo* using PC tumor xenograft mouse models and *ex vivo* after extracting vital organs and tumors. We are planning to publish our current and future results and discoveries in a peer-review journal.

4. IMPACT

What was the impact on the development of the principal discipline(s) of the project?
Proposed USPIO-5D3-DM1 drug delivery system with AL linkers will show minimal non-specific binding in healthy tissues providing a low systemic toxicity. After labeling this system with ^{89}Zr PET imaging tracer, it can be detected non-invasively by preclinical and translatable PET-MRI imaging system for the determination of biodistribution and tumor uptake, respectively. Hence, this study will provide an urgently needed experimental design that the PSMA-targeted theranostic system, USPIO-5D3-AL-DM1 can effectively reduce the tumor growth in primary and metastatic human PC xenograft mouse models. Image-guided drug delivery is expected to exhibit with a minimal off-target drug delivery and low systemic toxicity. Successful accomplishments of this project address the overarching challenges to: (a) develop treatments that improve outcomes for men with lethal prostate cancer; and (b) improve the quality of life for survivors of prostate cancer. This project will be significantly advantageous for the prostate cancer management of patients (45-60 years old service members and veterans) with both primary and metastatic prostate cancers. In fact, the knowledge achieved, and discoveries made by this project will be disseminated to researchers who are in the same field of medical research helping them to enhance the quality of their research.

What was the impact on other disciplines?
Nothing to Report

What was the impact on technology transfer?
Nothing to Report

What was the impact on society beyond science and technology?
Nothing to Report

5. CHANGES/PROBLEMS
Changes in approach and reasons for change:
We proposed to react amine and acidic linkers first and conjugated to the DM1 molecule in the original proposal. However, the amine-conjugated AL was unstable. Therefore, we changed the synthetic route to synthesize DM1-amine compound first and conjugated acidic linker and produce the DM1-AL. We have also studied the biodistribution in animal models using fluorescence labeled drug delivery system. This modification does not represent a significant change in the SOW of proposed project.
Actual or anticipated problems or delays and actions or plans to resolve them:
Covid-19 pandemic related issues and subsequent lock down of the university significantly delayed conduction this project. We have a delay of synthesizing compounds since some of commercial reagents and substrates were backordered for several months due to the Covid-19 pandemic. The freeze of hiring, backorder status of most of the chemicals and reagents, work at home and reduction of working time in the lab all had significant effect on the SOW schedule. We have planned an expedite work schedule to conduct the project for the incoming year focusing on the completion of drug delivery system, optimizing the radiolabeling and evaluating the therapeutic efficacy, pharmacokinetics, and biodistribution in prostate cancer xenograft mouse models.

Changes that had a significant impact on expenditures:
Due to the CoViD-19 outbreak, the project was significantly affected during the first one and half years of the project. The university activities of the Johns Hopkins School of Medicine have been shut down in March 2020. Phase 1 restart plan started in mid-June 2020; however, lab activities, and purchases were slowdown during Phase 1 and Phase 2 reopening sessions to keep low lab occupancy at this time. The hiring process was frozen for one year starting June 2020. We have hired a Research Technologist for 4 months (August 2021-November 2021) and conducted our research search focusing on HPLC characterization. We have selected a new candidate for this position and she will be joining the project in the near future.

Significant changes in use or care of human subjects, vertebrate animals, biohazards, and/or select agents:
Nothing to Report

Significant changes in use or care of human subjects:
Nothing to Report

Significant changes in use or care of vertebrate animals:
Nothing to Report

Significant changes in use of biohazards and/or select agents:
Nothing to Report

6. PRODUCTS

DM1-amine, a new compound
DM1-AL, a new compound

Publications, conference papers, and presentations

Journal publications:
1. Si G, Hapuarachchige S, Artemov D. Ultrasmall Superparamagnetic Iron Oxide Nanoparticles as Nanocarriers for Magnetic Resonance Imaging: Development and In Vivo Characterization ACS Applied Nano Materials, (Web):June 30, 2022, DOI: 10.1021/acsanm.2c01835 (https://pubs.acs.org/doi/10.1021/acsanm.2c01835). (Appendix 1)

Books or other non-periodical, one-time publications:
Nothing to Report

Other publications, conference papers, and presentations:
1. Development of USPIO-D1-5D3-CF750: An image-guided targeted drug delivery system for prostate cancer therapy. Sudath Hapuarachchige*, Ge Si, Catherine Foss, Cyril Barinka, Dmitri Artemov. ISMRM annual meeting, London, UK. (E-poster). (Appendix 2)
2. Optical- and MRI-detectable USPIO-5D3-DM1 nano-constructs for prostate cancer therapy. Sudath Hapuarachchige*, Ge Si, Cyril Barinka, Dmitri Artemov. (WMIC annual meeting, Miami, FL, USA. (Abstract submitted). (Appendix 3)

Website(s) or other Internet site(s):
Nothing to Report
Technologies or techniques:
Nothing to Report
Inventions, patent applications, and/or licenses:
Nothing to Report

Other Products:
Nothing to Report

7. PARTICIPANTS & OTHER COLLABORATING ORGANIZATIONS

What individuals have worked on the project?

Name:	Sudath Hapuarachchige, PhD	Catherine Foss, PhD	Dmitri Artemov, PhD	Deaven Avery
Project Role:	Principle Investigator (PI)	Co-Investigator	Co-Investigator	Research Technologist
Researcher Identifier (ORCiD)	0000-0002-1166-8247	0000-0001-8870-5993	0000-0002-6837-8953	-
Nearest person month worked:	6.0	2.4	1.2	12 (*For 4 months*)
Contribution to Project:	Development of USPIO-5D3-DM1 drug delivery systems. In vitro and *in vivo* imaging. Supervising and ensuring stable workflow	Development of USPIO-5D3-DM1-DFO and ^{89}Zr radiolabeling.	MRI imaging and image processing	Maintaining cells and research animals, characterization of compounds.
Funding Support:	DoD/Emerson Collective	DoD/NIH-NCI	DoD/NIH-NCI	*This award*

Has there been a change in the active other support of the PD/PI(s) or senior/key personnel since the last reporting period?

Nothing to Report

What other organizations were involved as partners?

Nothing to Report

8. SPECIAL REPORTING REQUIREMENTS

COLLABORATIVE AWARDS:

Nothing to Report

QUAD CHARTS:

Nothing to Report

9. APPENDICES

1. Article published in ACS Applied Nano Materials
2. Abstract submitted for the annual meeting of ISMRM held in London, UK.
3. Abstract submitted for the annual meeting of WMIC held in Miami, Florida, USA.

ACS APPLIED NANO MATERIALS

www.acsanm.org Article

Ultrasmall Superparamagnetic Iron Oxide Nanoparticles as Nanocarriers for Magnetic Resonance Imaging: Development and *In Vivo* Characterization

Ge Si, Sudath Hapuarachchige, and Dmitri Artemov*

Cite This: https://doi.org/10.1021/acsanm.2c01835 Read Online

ACCESS | Metrics & More | Article Recommendations | Supporting Information

ABSTRACT: Ultrasmall superparamagnetic iron oxide nanoparticles (uSPIOs) are attractive platforms for the development of smart contrast agents for magnetic resonance imaging (MRI). Oleic acid-capped uSPIOs are commercially available yet hydrophobic, hindering *in vivo* applications. A hydrophilic ligand with high affinity toward uSPIO surfaces can render uSPIOs water-soluble, biocompatible, and highly stable under physiological conditions. A small overall hydrodynamic diameter ensures optimal pharmacokinetics, tumor delivery profiles, and, of particular interest, enhanced T_1 MR contrasts. In this study, for the first time, we synthesized a ligand that not only fulfills the as-proposed properties but also provides multiple reactive groups for further modifications. The synthesis delivers a facile approach using commercially available reactants, with resultant uSPIO−ligand constructs assembled through a single-step ligand exchange process. Structural and molecular size analyses confirmed size uniformity and small hydrodynamic diameter of the constructs. On average, 43 reactive amine groups were present per uSPIO nanoparticle. Its r_1 relaxivity has been tested on a 7 Tesla MR instrument and is comparable to that of the clinically available T_1 gadolinium-based contrast agent GBCA (1 vs 3 mM^{-1} s^{-1}, respectively). A significant decrease in tumor T_1 (15%) within 1 h of injection and complete signal recovery after 2 h were detected with a dose of 7 μg Fe/g mouse. The agent also has high r_2 relaxivity and can be used for T_2 contrast-enhanced MRI. Taken together, good relaxation and delivery properties and the presence of multiple surface reactive groups can facilitate its application as a universal MRI-compatible nanocarrier platform.

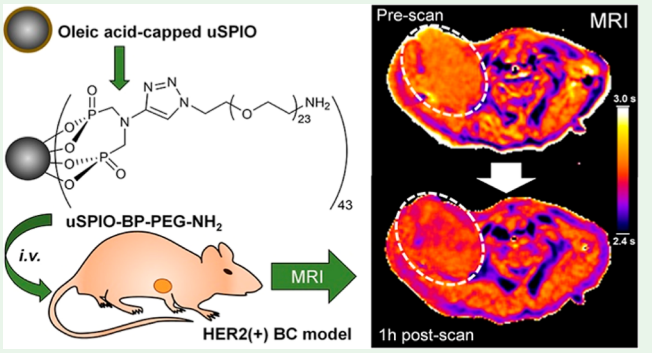

KEYWORDS: *uSPIO, contrast agent, preclinical cancer models, click chemistry, ligand exchange, T_1-/T_2-weighed imaging, MRI*

INTRODUCTION

Magnetic resonance imaging (MRI) has been a staple in medical imaging since its launch in 1971. Compared to other non-invasive clinical imaging modalities, such as computed tomography (CT), positron emission tomography (PET), single photon emission computed tomography (SPECT), or ultrasound, MRI provides excellent soft-tissue contrast with great spatial resolution and minimal safety issues due to its non-radioactive nature. Various imaging acquisition sequences have been introduced, however, T_1- and T_2-weighed images remain the most prevalent. Although T_2-weighed images provide high endogenous contrasts, exogenous contrast agents that typically produce positive T_1 contrast enhancement that results in images with increased intensities are preferable for diagnostic imaging.

Currently, the only type of FDA-approved MRI contrast agents is gadolinium-based contrast agents (GBCAs). However, patients suffer from potential side effects such as nephrogenic system fibrosis, hypertension, kidney failure, and so forth caused by GBCAs. Importantly, they may also accumulate non-specifically in the brain and lack convincing patient screening protocol.[1] Iron oxide nanoparticles (IONPs) have been clinically used for the treatment of anemia. IONPs are non-toxic, naturally degradable after administration, and eventually become a source for *in vivo* iron supplements. Nanoscale superparamagnetic IONPs (SPIO), with a typical core size of 20−50 nm, have long been exploited as T_2 contrast agents for MRI. Intriguingly, when the SPIO core size is decreased to below ∼5 nm, it starts exhibiting increased T_1 enhancement due to the following reasons: (1) a high surface to volume ratio exposes multiple Fe^{2+}/Fe^{3+} ions to water protons diffused through the hydrophilic layer and shortens

Received: April 27, 2022
Accepted: June 17, 2022

https://doi.org/10.1021/acsanm.2c01835
ACS Appl. Nano Mater. XXXX, XXX, XXX−XXX

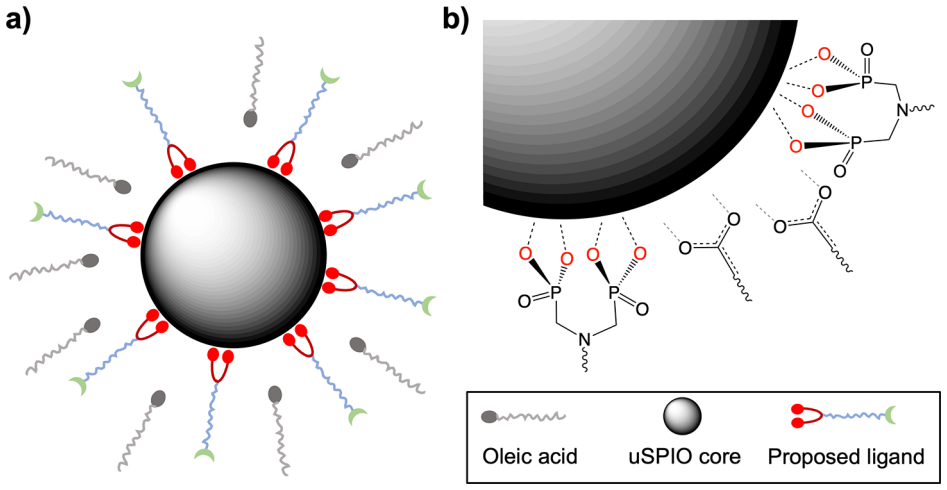

Figure 1. Schematic diagram of the uSPIO and ligand exchange process. (a) Proposed ligand competes against the innate OA ligand during the ligand exchange process. (b) Close-up look at the uSPIO core surface: the proposed ligand with four coordination sites per molecule strongly binds with the core surface displacing the innate OA ligand.

their longitudinal relaxation time by providing empty orbits; (2) short correlation time of ultrasmall nanoparticles also favors T_1 relaxation processes.[2] Multiple studies using sub-5 nm ultrasmall SPIOs (uSPIO) have shown promising T_1 enhancement patterns.[3,4]

uSPIOs can be synthesized via multiple methods such as hydrolysis, thermolysis, and microwave or one-pot synthesis.[5] Among them, thermolysis produces uSPIOs with the most uniform size with the least polydisperse index (PDI) and is commercially available for a low cost.[6,7] However, uSPIOs produced by such an approach are naturally hydrophobic and are typically stabilized with an oleic acid (OA) surface ligand in non-polar organic solvents (e.g., $CHCl_3$) to prevent aggregation. Therefore, a post-synthesis surface modification process to render uSPIOs hydrophilic and biocompatible is necessary for *in vivo* applications. There are two major approaches to render a hydrophobic uSPIO hydrophilic: ligand encapsulation and ligand exchange.[8−10] Ligand encapsulation uses an amphiphilic ligand, where the hydrophobic part is embedded in the OA layer, while the hydrophilic part caps the outer surface for stabilization in water-based solvents. Ligand exchange allows a water-soluble ligand to completely replace the OA layer. The water-soluble ligand is dissolved in a solvent that is miscible with the solvent containing hydrophobic uSPIO−OA particles. Due to a stronger affinity of the hydrophilic ligand to the uSPIO surface than OA, OA is stripped off the uSPIO surface and replaced by the ligand. The latter approach allows using of smaller molecular-weight ligands, and the resulting hydrophilic uSPIO nanoparticles have smaller hydrodynamic diameter (HD) with improved biocompatibility for *in vivo* delivery.

The major drawback of the ligand encapsulation method is that the densely packed hydrophobic layer prevents the diffusion of water molecules to the uSPIO core surface, thus reducing T_1 relaxivity of the agent. Since ligand exchange uses hydrophilic compounds, water molecules can travel close enough for surface iron to foster longitudinal relaxation. Therefore, in this report, we used the ligand exchange approach to produce a stable, hydrophilic uSPIO−ligand construct with high T_1 relaxivity optimized for contrast-enhanced MRI.

One important application of contrast-enhanced MRI is cancer imaging. Early detection and diagnosis of cancers are highly important due to the rapid progressive nature of aggressive tumors. To generate detectable MR contrast, a significant amount of the contrast agent needs to accumulate in the region of interest (ROI). The enhanced permeability and retention (EPR) effect due to the leaky tumor vasculature allows passive accumulation of sub-100 nm nanoparticles.[11−13] Specific protein upregulation or surface protein overexpression in the tumor microenvironment can be used for targeted delivery by specific binding and accumulation of the contrast agent at the target.[13,14] Target-specific delivery requires the nanoscale contrast agent to bear surface functional groups for modification with high-affinity targeting moieties. A small overall HD is preferred for the optimal tumor delivery.[15] Hence, to design a water-soluble uSPIO as a T_1 contrast agent that fulfills as-proposed properties, a ligand should consist of the following three domains (Figure 1a): (1) an anchor that has strong affinity toward the uSPIO surface; (2) a hydrophilic layer that renders uSPIOs stable in water-based solvents; and (3) a reactive group that allows further modification for targeted delivery and therapy.

Molecules that have paired electrons as electron donors to uSPIO surface ions Fe^{2+}/Fe^{3+} with a compatible orbit geometry can be a potential anchor group choice. Successful use of various groups including carboxylic groups, catechol groups, bisphosphonate groups and large molecules such as dextran or oligosaccharides has been reported.[16−24] Catechol and bisphosphonate groups provide the strongest affinity, thus producing more stable uSPIO constructs. However, the binding affinity of catechol groups with $Fe^{2+/3+}$ is too strong, which can lead to the disassembly of the uSPIO.[25−27] Bisphosphonate groups are clinically used to treat osteoporosis and cancer metastasis in bone.[28] They are non-toxic and have proper coordination geometry to the IONP surface which results in an appropriate affinity that is strong enough to stabilize uSPIOs without causing degradation of the core.[28,29] A staple choice for the biocompatible hydrophilic layer is polyethylene glycol (PEG) that can also protect the nanoparticle from recognition by the host immune system.[30] Hetero-bifunctional PEG linkers of high purity (>95% pure) are commercially available. These reactive groups provide facile

https://doi.org/10.1021/acsanm.2c01835
ACS Appl. Nano Mater. XXXX, XXX, XXX−XXX

Scheme 1. Synthesis of Bisphosphonate-Anchored uSPIOs

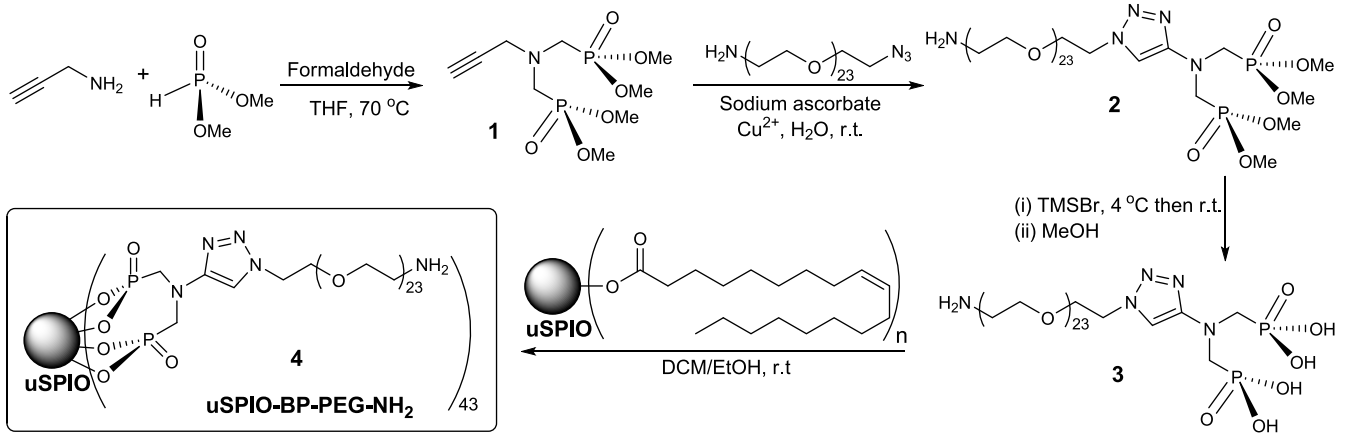

modification with high yield via amine conjugation, which remains one of the most versatile bioconjugation reactions under mild conditions.[31] Therefore, a bisphosphonate anchor group with a hydrophilic PEG chain and amine reactive group makes an ideal anchor.

In this study, we focused on the synthesis of such a proposed ligand and uSPIO construct. Characterizations confirmed the intended structure and long-term stability. MRI of phantoms with various uSPIO concentrations was used for T_1 and T_2 calculations. *In vivo* MRI was performed in tumor-bearing mice injected with uSPIOs. Tissue distribution and clearance of uSPIOs were determined, and tumor signal enhancement was evaluated using quantitative pixel-by-pixel relaxation mapping. Here, we describe the synthesis of the ligand and the ligand exchange method to produce a stable, water-soluble uSPIO−ligand construct with a small HD, good *in vivo* tumor delivery properties, and optimized MR T_1 enhancement.

EXPERIMENTAL SECTION

Materials. The PEG linker azido-PEG23 amine (BP-21956) was purchased from BroadPharm. The OA-capped uSPIO (5 nm core size, 25 mg/mL in $CHCl_3$) was purchased from Ocean NanoTech. All other chemicals, solvents, and materials of analytical grade were purchased from MilliporeSigma. The synthesis steps are presented in Scheme 1.

Methods. *Synthesis of Tetramethyl (Prop-2-ynylazanediyl)bis-(methylene)diphosphonate (**1**).* The anchor was synthesized by the modified Kabachnik−Fields reaction (Scheme 1).[32−34] Briefly, a solution of 37% formaldehyde (0.93 mL, 10 mmol) was mixed with tetrahydrofuran (THF) (5 mL) in a round bottom flask. Temperature was brought down to 4 °C using an ice bath. The mixture was stirred, and propargyl amine (0.32 mL, 5 mmol) was added dropwise over 15 min. Then, the temperature was gradually brought back to room temperature. To the mixture, dimethyl phosphite (0.92 mL, 10 mmol) was added dropwise. The reaction solution was slowly heated up using an oil bath to reflux. After 12 h, solvents were evaporated using a rotovap under reduced pressure. A maroon-color solid residue was dissolved in $CHCl_3$; then, the organic layer was washed with a 1N NaOH solution and then dried with anhydrous Na_2SO_4. The organic solvent was evaporated using a rotovap under reduced pressure. The yellow-color crude product was purified by column chromatography (CH_2Cl_2/MeOH = 49:1) to obtain the pure product as a light-yellow oil (1.06 g, 72%). The product was characterized by ^{1}H NMR, ^{13}C NMR, ^{31}P NMR, and mass spectrometry (LCQ-Fleet).

^{1}H NMR spectroscopy (500 MHz, $CDCl_3$, δ): 3.81 (12H, d, J = 10.7 Hz, −OCH_3), 3.77 (2H, s, N−CH_2−alkyne), 3.13 (d, J = 11.25 Hz, 4H, N−CH_2−P), 2.32 (1H, s, alkyne-H). ^{13}C NMR (500 MHz, $CDCl_3$, δ): 74.46, 52.96, 50.00, 48.65, 45.54. ^{31}P NMR (500 MHz, $CDCl_3$, δ): 25.90. Mass spectrometry (LCQ-Fleet) m/z: [M+Na^+] = 321.9 (M = 298.9, calculated).

*Synthesis of Tetramethyl {[1-(PEG23)-1H-1,2,3-triazol-5-yl]-methylazanediyl}bis(methylene) Diphosphonate (**2**).* A mixture of dry compound **1** (62.4 mg, 0.21 mmol) and azido-PEG23 amine (180.5 mg, 0.16 mmol) in a round bottom flask was stirred and completely dissolved in deionized water (5 mL). Then, $CuSO_4{\cdot}5H_2O$ (2.2 mg, 8.8 μmol) and (+)-sodium L-ascorbate (10.5 mg, 0.053 mmol) were added to the reaction mixture. The reaction solution was stirred at room temperature overnight. The solvent of the bright-yellow reaction mixture was removed by lyophilization. The crude product was redissolved in 4 °C THF and then filtered through a hydrophobic polytetrafluoroethylene (PTFE) filter to remove catalysts and other insoluble impurities. Excess THF was then added to the filtered crude, and temperature was dropped to −20 °C to precipitate the product. Two rounds of precipitation yielded an orange−red product (229.7 mg, 83%). The product was characterized by ^{1}H NMR, ^{13}C NMR, and mass spectrometry.

^{1}H NMR (500 MHz, $CDCl_3$, δ): 7.89 (2H, s, −NH_2), 7.77 (1H, s), 4.54 (2H, t, J = 5.05, 5.10 Hz), 4.14 (2H, s), 3.92 (2H, s), 3.88 (2H, t, J = 5.15, 5.05 Hz), 3.78 (12H, d, J = 10.65 Hz, −OCH_3), 3.69−3.61 (96H, m, CH_2−CH_2−O−), 3.19 (5H, d, J = 10.3 Hz, −N−CH_2−P). ^{13}C NMR (500 MHz, $CDCl_3$, δ): 143.03, 124.59, 70.52−69.47, 66.76, 52.76, 51.08, 50.23, 49.58, 48.30, 40.38. ^{31}P NMR (500 MHz, $CDCl_3$, δ): 26.59. Mass spectrometry (LCQ-Fleet) m/z: [M+2H^+] = 700.1 (M = 1398.2, calculated).

*Synthesis of Diphosphonic Acid {[1-(71-Amino-PEG23)-1H-1,2,3-triazol-5-yl]methylazanediyl} Bis(methylene) (**3**).* Dry compound **2** (140.0 mg, 0.10 mmol) was dissolved in anhydrous dichloromethane (DCM, 5 mL) under argon in a round bottom flask. The temperature of the mixture was brought down to 4 °C in an ice bath. To the reaction mixture, bromotrimethylsilane (TMS-Br, 132 μL, mmol) was added dropwise and stirred continuously in an ice bath. After 15 min, the temperature was gradually brought back to room temperature, and the reaction was carried out under argon overnight. The reaction mixture was rotovaped under reduced pressure to remove the solvent and excess TMS-Br. The crude product was redissolved in methanol (MeOH, 5 mL), and the solution was stirred for 5 h. The solvent was removed using a rotovap, and the product was dried under high vacuum. The product was redissolved in water and lyophilized to obtain a dark-red ligand, **3** (210.3 mg, 95.5% yield. Overall yield 57.1%). The product was stored at −20 °C.

^{1}H NMR (500 MHz, $CDCl_3$, δ): 7.47, 7.29 (4H, s, −NH_2), 3.70−3.66 (96 H, m, CH_2−CH_2−O−), 3.51−3.45 (2H, m), 3.24 (2H, s). 1.99 (2H, t, J = 7.0 Hz), 1.73 (2H, t, J = 7.5 Hz), 1.43 (6H, s). ^{13}C NMR (500 MHz, $CDCl_3$, δ): 135.76, 128.23, 125.50, 70.50−69.92, 66.78, 40.43, 34.03, 30.94, 30.31, 29.23, 21.17. ^{31}P NMR (500 MHz, $CDCl_3$, δ): 10.98. Mass spectrometry (LCQ-Fleet) m/z: [M+2H^+] = 671.7 (M = 1341.4, calculated).

*Ligand Exchange of the uSPIO (**4**).* The OA-capped uSPIO (Fe: 1 mg) in chloroform (40 μL) was dispersed in anhydrous DCM (0.5

https://doi.org/10.1021/acsanm.2c01835
ACS Appl. Nano Mater. XXXX, XXX, XXX−XXX

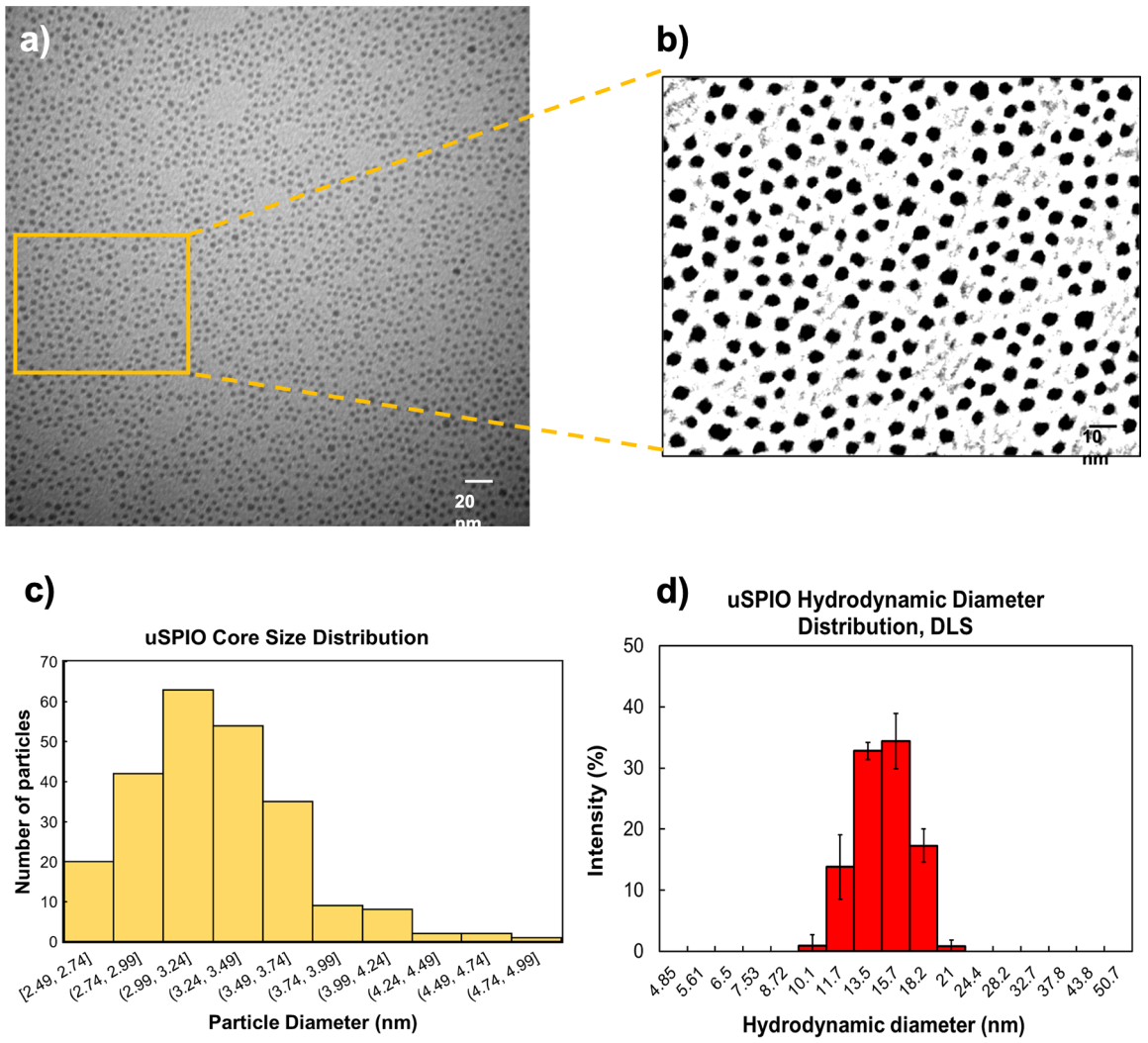

Figure 2. Determination of the size of uSPIO-BP-PEG-NH_2 with TEM and DLS. (a–c) TEM images and size distribution: (a) whole FOV under 400k magnification. The ROI for analysis is highlighted in a red square near left center; (b) analyzed nanoparticles; and (c) uSPIO core size distribution by TEM. (d) uSPIO HD distribution by DLS, averaged over four measures. Error bars indicate standard deviation among these measurements.

mL). Then, ligand compound **3** (3.0 mg) in 200 proof ethanol (EtOH, 0.5 mL) was added, and the mixture was stirred overnight. Excess hexane was added to the reaction mixture to precipitate hydrophilic uSPIOs. Precipitated uSPIOs were isolated by ultracentrifugation (30 kDa MWCO, 4500 rpm, 5 min). The uSPIO product was observed as a dark-brown pellet at the bottom of the centrifuge tube. It was re-solubilized with 1 mL of double-distilled water, followed by filtration through a 0.45 μm hydrophilic PTFE filter unit. No aggregate was observed during this process. The excess ligand was filtered, and the uSPIO was concentrated by ultracentrifugation (30 kDa MWCO, 1500 rpm, 25 min) three times. The water-soluble uSPIO product uSPIO-BP-PEG-NH_2 was stored at 4 °C in water or phosphate buffered saline (PBS) solution.

Characterization of uSPIO-BP-PEG-NH_2. The OA-capped uSPIO, unpurified uSPIO-BP-PEG-NH_2, filter-purified USPIO-OH-NH_2, and three-round centrifuged uSPIO-BP-PEG-NH_2 core sizes were measured with transmission electron microscopy (TEM). To prepare TEM grids, a concentration of 150–200 μg/mL Fe was used, followed by staining with 1% neutral phosphotungstic acid. Images were acquired at 400k magnification using a Hitachi 7600 transmission electron microscope. Image analysis on all uSPIO constructs was performed using ImageJ-Fiji software. HD of water-soluble uSPIO-OH-NH_2 was measured using dynamic light scattering (DLS). A concentration of 1.0 mg/mL of uSPIOs in PBS was used for measurement. Zeta potential was measured using a capillary zeta cell with a concentration of 2.0 mg/mL of uSPIOs in PBS, at pH = 7.0. Fourier-transform infrared (FT-IR) spectra of the OA-capped uSPIO, uSPIO-BP-PEG-NH_2, and final ligand BP-PEG-NH_2 were obtained using a Thermo Nicolet Nexus 670 FTIR spectrometer with an attenuated total reflection accessory. 2 mg of Fe or 4 mg of the ligand in 50 μL of water or ethanol droplets were used for sampling. Background was taken before each measurement and was subtracted to obtain final spectra.

In Vitro MRI Phantom Study and the Determination of Relaxivity. Longitudinal and transverse relaxivities (r_1 and r_2) of uSPIO-BP-PEG-NH_2 were measured on a 7 T horizontal bore Bruker Biospec MR scanner using phantoms containing a concentration series of uSPIO-BP-PEG-NH_2 embedded in 3% agarose in PBS (0.18, 0.45, 0.90, 1.43, and 1.79 mmol/L). Phantoms with different uSPIO concentrations were arranged in a holder within a volume MR coil (inner diameter of 74 mm). The ROI was chosen to produce uniform images in the center of phantoms using a slice thickness of 2 mm. T_1 maps were acquired with a Rapid Acquisition with Relaxation Enhancement (RARE) Fast Spin-Echo sequence, with time to echo (T_E) set at 13 ms and varying repetition time (T_R) at 755, 1000, 1500, 2000, 4000, and 8000 ms, at an in-plane resolution of 0.25 mm. T_2 maps were acquired with the RARE fast spin-echo sequence, with varying T_E at 6.5, 10, 12.5, 15, 20, and 25 ms and TR set at 5000 ms.

https://doi.org/10.1021/acsanm.2c01835
ACS Appl. Nano Mater. XXXX, XXX, XXX–XXX

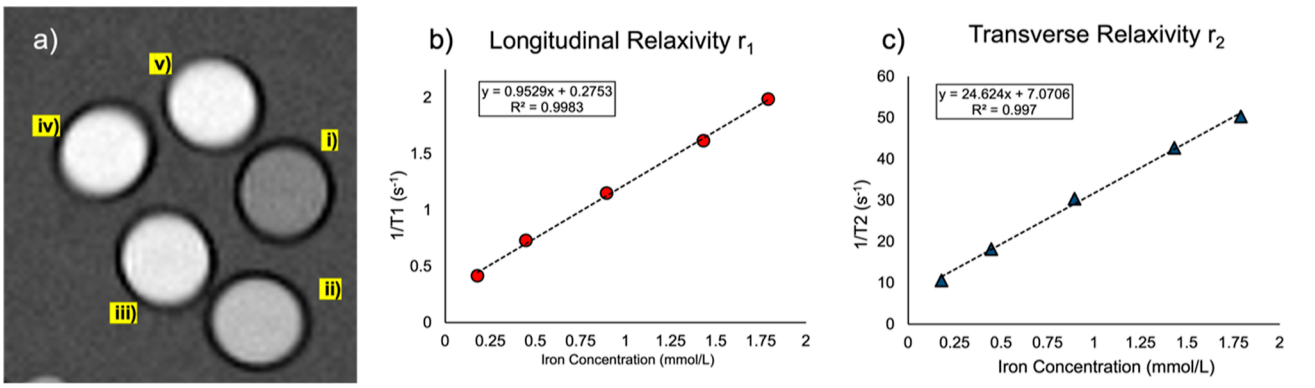

Figure 3. Phantom imaging and the calculation of relaxivity. (a) Phantom image of uSPIO-BP-PEG-NH_2 at T_E = 13 ms and T_R = 1000 ms. uSPIOs are embedded in 3% agarose gels with various concentrations i–v: 0.01; 0.02; 0.05; 0.08; and 0.1 mg/mL. Units have later been converted to mmol/L for relaxivity calculations; (b) r_1 measurements. An average T_1 for each concentration was calculated, and $1/T_1$ was plotted against the iron concentration in mmol/L. r_1 is defined as the slope value; and (c) r_2 measurements. Similarly, average T_2 for each concentration was calculated, and $1/T_2$ was plotted against the iron concentration. The slope value is r_2.

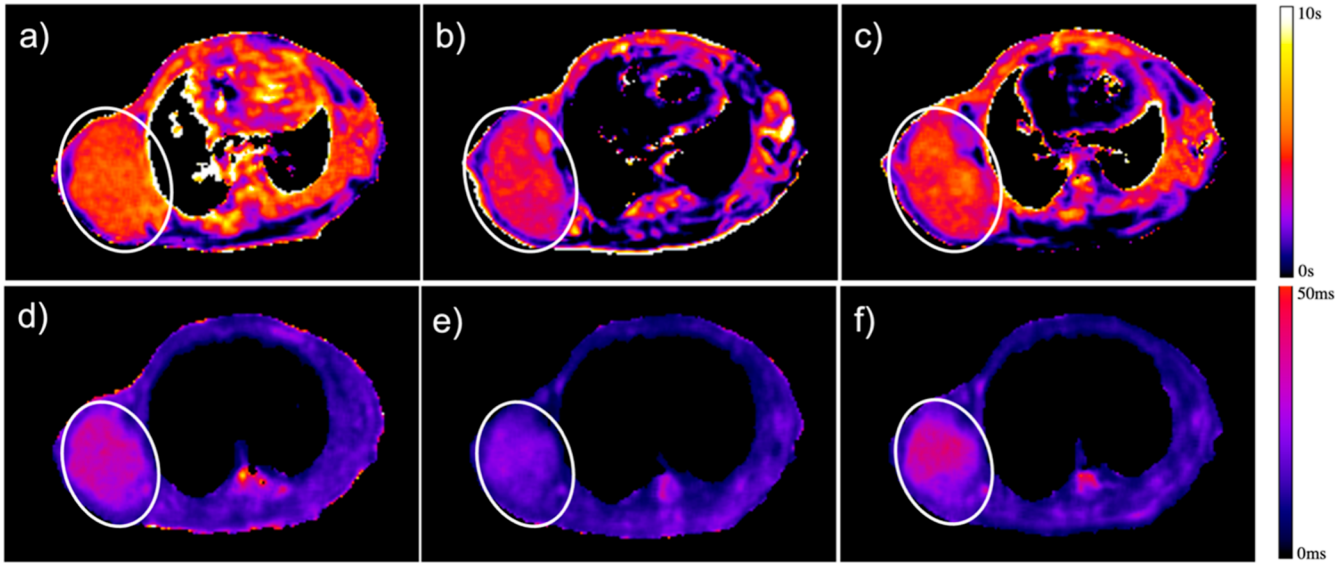

Figure 4. Quantitative T_1 and T_2 maps of the uSPIO with tumor regions highlighted with white ovals. (a–c) T_1 mapping of the uSPIO in the mouse: (a) pre-injection; (b) 30 min post-injection; and (c) 4 h post-injection. (d–f) T_2 mapping of the uSPIO in the mouse: (d) pre-injection; (e) 30 min post-injection; and (f) 4 h post-injection.

Quantitative pixel-by-pixel T_1 and T_2 maps were reconstructed using IDL software developed in our laboratory. Mean pixel intensity was used for calculation. For longitudinal relaxation, the equation $M = M_0(1 - e^{-T_R/T_1})$ for saturation recovery was used to determine T_1 at each concentration, and r_1 was determined from a linear regression analysis of plots for $1/T_1$ against iron concentrations. For transverse relaxation, equation $M = M_0e^{-T_E/T_2}$ was used to determine T_2 and r_2.

Mouse Models. BT-474 breast cancer cells (ATCC) were grown in 46-X medium supplemented with 10% fetal bovine serum (Sigma), 100 units/mL penicillin, and streptomycin for inoculation of 6–8 week old athymic Nu/Nu female mice (Charles River Laboratories). An estrogen pellet 17β-estradiol (0.72 mg, 90 day release, Innovative Research of America) was implanted in the subdermal area on the back of each mouse 24 h prior to inoculation. BT-474 cells (2×10^6 cells in 50 μL of 50% of Matrigel/media) were inoculated into the second mammary fat pad of the mouse.

MR Imaging of Breast Cancer Xenograft Mouse Models Using uSPIOs. After the tumor had grown to 200–300 mm^3 in size, uSPIO-BP-PEG-NH_2 (280 μg Fe/kg dose in 200 μL of saline) was administrated by tail-vein injection. Prior to injection, uSPIO-BP-PEG-NH_2 was sterilized by filtration through 0.22 μm polyvinylidene difluoride filter units. filters. Mice were imaged using T_1- and T_2-weighted sequences as described above before and at 30 min, 1, 2, and 4 h post-injection. All animals were sacrificed immediately after imaging. Tissues were harvested and lyophilized to determine the uSPIO-BP-PEG-NH_2 uptake by inductively coupled plasma mass spectrometry (ICP–MS).

RESULTS AND DISCUSSION

Synthesis and Ligand Exchange. The ligand was synthesized by a simple approach at room temperature and normal pressure. The starting materials and reagents used are commercially available. Click chemistry, such as copper-catalyzed alkyne–azide cycloaddition (CuAAC), has significantly simplified the PEG-anchor conjugation and purification process while affording a high yield.[35,36] The final ligand is stable at −20 °C for at least 2 years. The uSPIO–ligand construct is stable in water or PBS for at least 3 months without an aggregation or significant changes in size.

Size, Zeta Potential, and FT-IR of uSPIO-BP-PEG-NH_2. At least 200 particles in one continuous TEM ROI were measured for an average core size. The resulting average core

https://doi.org/10.1021/acsanm.2c01835
ACS Appl. Nano Mater. XXXX, XXX, XXX–XXX

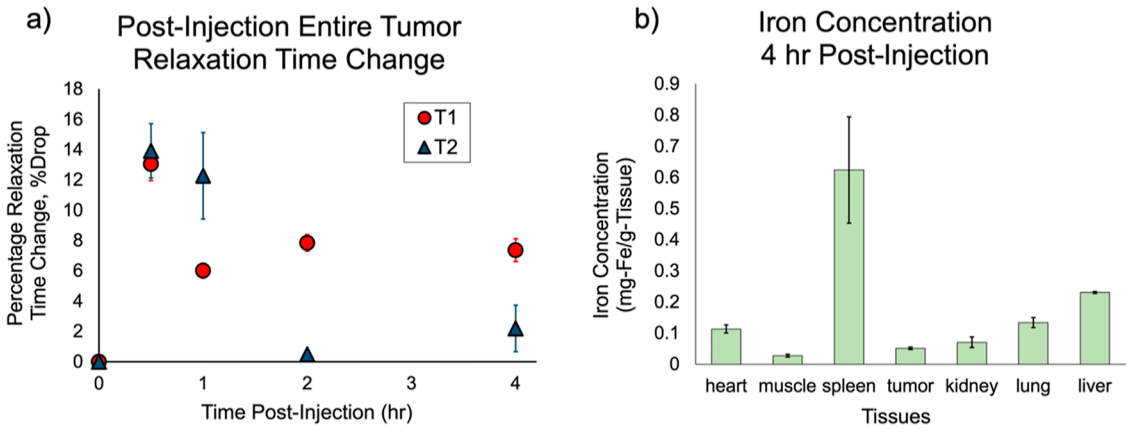

Figure 5. (a) Tumor relaxation time change, % drop $= -\frac{T_{\text{time point}} - T_{\text{pre-injection}}}{T_{\text{pre-injection}}} \times 100\%$. Error bars calculated from results for four different animals. Note that the error bar on T_2 at the 2 h time point does exist, even though it seems invisible due to the small error. (b) Tissue iron concentration ($N = 3$ mice, unit in mg Fe/g tissue). Each mouse was injected with 200 μL of the uSPIO at a 1 mg Fe/mL concentration (around 7μg Fe/g mice). Mice were sacrificed 4 h post-injection. Organs were harvested and weighed before snap-frozen and being lyophilized for ICP−MS analysis. ICP−MS analysis has passed all QC standards with a 99% recovery rate.

size of the final uSPIO construct was 3.3 nm (Figure 2a−c). Additionally, core size analysis was also done on OA-capped uSPIOs, unpurified uSPIO-BP-PEG-NH_2, and filter-purified uSPIO-OH-NH_2 (Supporting Information S2), showing a similar core size of the final construct (3.4, 3.3, and 3.3 nm, respectively). This has proved that neither the ligand exchange process nor any of the purification steps have caused considerable size change. DLS measurement showed an HD of 14.5 nm with a PDI width of 0.1 (Figure 2d). It also remained unchanged for at least 3 months. Zeta potential is at +11.8 mV at pH = 7.0, suggesting a net positive net charge (Supporting Information S2.4). FT-IR spectra show a P−O stretching at 1100 cm^{-1} on both the ligand and uSPIO post-ligand exchange yet not appearing in OA-capped uSPIOs, suggesting the presence of a synthesized ligand on hydrophilic uSPIOs after ligand exchange (Supporting Information S2.3).

MR Imaging. Phantom imaging was performed to determine the r_1 and r_2 relaxivities of uSPIOs (Figure 3). At 7 T, the calculated r_1 and r_2 relaxivities were 0.95 and 29.16 mM^{-1} s^{-1}, respectively. Most of the literature-reported relaxivity data on IONP constructs are measured on 1.5 or 3 T clinical MRI scanners. Here, we measured the relaxivity on a preclinical 7 T MRI instrument, as we envision further extensive testing and applications of the agent in preclinical animal models using high-field MRI. Within the past several years, 7 T clinical MR scanners have also become available for clinical research.[37] FDA-approved GBCA T_1 contrast agents typically have an r_1 relaxivity of around 3.00 mM^{-1} s^{-1} and an r_2 value of 15.00 mM^{-1} s^{-1}.[38,39] Although this uSPIO construct has lower relaxivity than GBCAs,[40] the uSPIO by nature is non-toxic. Moreover, since GBCAs are small molecules, no further modifications can be made without significantly altering their physical or chemical properties. On the contrary, the uSPIO-BP-PEG-NH_2 construct provides 43 amine functional groups per nanoparticle on the surface (Supporting Information S3) for further modifications via standard amine bioconjugate chemistry with high yield and minimal, non-toxic side products that can be easily purified while retaining its key physical and chemical properties.

In vivo injection of uSPIOs into BT-474 tumor-bearing mice ($N = 4$) was performed to investigate the uSPIO tissue distribution and clearance. Pixel-by-pixel relaxation maps revealed that the uSPIO has induced a 15% increase in both T_1 and T_2 contrasts around 30 min to 1 h post-injection (Figure 4b,e) and has recovered to ∼95% contrast 4 h post-injection (Figure 4c,f). ICP−MS analysis has also confirmed that at 4 h post-injection, most iron has cleared out from the tumor, with practically all iron trapped in the liver and spleen (Figure 5, corresponding gray-scale images, see Supporting Information S4).

A rapid accumulation of uSPIOs in the tumor region, presumably due to the EPR effect, was detected within 30 min after injection. The maximum contrast enhancement was observed at the 1 h post-injection time point. Small-diameter uSPIOs and surface iron ions that provide two−three empty orbits per iron (Fe^{2+} or Fe^{3+}) induce efficient T_1 relaxation in water molecules. The densely packed PEG ligand allows water molecules in nearby tissues to diffuse to the iron core and interact with iron's empty orbits. T_2 changes in the tumor regions with uSPIO accumulation are likely due to the local field in homogeneities generated by uSPIO nanoparticles. We also observed a rapid clearance of untargeted small-HD uSPIO constructs from the tumor within 4 h. Combined with its high relaxivity, this makes it a good candidate as a universal nanocarrier platform for MRI-based applications with an optimal delivery profile.

CONCLUSIONS

We have demonstrated a facile approach to synthesize a hydrophilic ligand that has high affinity and good stability for sub-5 nm uSPIOs, and the resulting uSPIO-BP-PEG-NH_2 construct has shown excellent T_1 and T_2 relaxation enhancement properties in phantoms and *in vivo* in experimental animal models. Most tumor regions showed an enhanced signal within the first hour post-injection and had restored 90−95% relaxivity 2−4 h post-injection. 4 and 24 h post-injection ICP−MS analysis has shown that the tumor iron levels were low, while the liver and spleen showed elevated iron accumulation. Based on extensive published studies,[41] it is proposed that the iron in these tissues will be slowly digested and metabolized as iron supplements, without causing toxicity.

https://doi.org/10.1021/acsanm.2c01835
ACS Appl. Nano Mater. XXXX, XXX, XXX−XXX

The reproducible, cost-friendly, and simple synthesis approach of the ligand allows for a staple starting point for further modification. The resultant uSPIO construct is nontoxic and stable with high r_1 relaxivity and thus can potentially be translated to clinical MRI use. The ample modification sites of this uSPIO−ligand construct allow further *ex vivo* or *in vivo* modifications via simple bioconjugate reactions. For example, if conjugated with a chelator for radioactivity, this construct can be readily employed on a PET−MRI instrument for simultaneous dual-modality imaging. Specific protein markers that up-regulate in early cancer can be a sign for early cancer development. High-affinity molecules for such proteins can be conjugated to the uSPIO construct resulting in selective and specific accumulation at the tumor site, enabling early cancer detection and diagnosis. Hence, the uSPIO-BP-PEG-NH_2 construct can be used a theranostic platform for imaging-guided targeted drug delivery.

■ ASSOCIATED CONTENT

Supporting Information

The Supporting Information is available free of charge at https://pubs.acs.org/doi/10.1021/acsanm.2c01835.

NMR and mass spectrometry spectra of each product in the ligand synthesis process, TEM images of uSPIOs in each step of ligand exchange and purification, calculation of the number of reactive amine groups per nanoparticle, and gray-scale *in vivo* MR images (PDF)

■ AUTHOR INFORMATION

Corresponding Author

Dmitri Artemov − *The Russell H. Morgan Department of Radiology and Radiological Science, School of Medicine, The Johns Hopkins University, Baltimore, Maryland 21205, United States; Department of Oncology, the Sidney Kimmel Comprehensive Cancer Center, School of Medicine, The Johns Hopkins University, Baltimore, Maryland 21287, United States;* orcid.org/0000-0002-6837-8953; Phone: +1(410) 614-2703; Email: dartemo2@jh.edu

Authors

Ge Si − *Department of Chemical and Biomolecular Engineering, The Johns Hopkins University, Baltimore, Maryland 21218, United States; The Russell H. Morgan Department of Radiology and Radiological Science, School of Medicine, The Johns Hopkins University, Baltimore, Maryland 21205, United States;* orcid.org/0000-0003-1554-6551

Sudath Hapuarachchige − *The Russell H. Morgan Department of Radiology and Radiological Science, School of Medicine, The Johns Hopkins University, Baltimore, Maryland 21205, United States; Department of Oncology, the Sidney Kimmel Comprehensive Cancer Center, School of Medicine, The Johns Hopkins University, Baltimore, Maryland 21287, United States;* orcid.org/0000-0002-1166-8247

Complete contact information is available at: https://pubs.acs.org/10.1021/acsanm.2c01835

Author Contributions

D.A. and S.H. conceptualized the delivery strategy and designed the study. G.S. designed, synthesized, and characterized the compounds and nanoparticles and conducted the phantom and *in vivo* study. S.H. assisted with the synthesis and characterization of compounds. G.S. and D.A. processed MRI images. D.A. guided and supervised the project. G.S. wrote the manuscript with input and approval from all other authors.

Funding

This study was supported by NIH/NCI (R01CA209884, D.A.) and, in part, by DOD/CDMRP (W81XWH-20-1-0429, S.H.).

Notes

The authors declare no competing financial interest.

■ ACKNOWLEDGMENTS

The authors acknowledge Desmond Jacob and Rui Chen for the assistance with MRI and ICP−MS analysis, respectively.

■ ABBREVIATIONS

CT, computed tomography
DCM, dichloromethane
DLS, dynamic light scattering
EPR, enhanced permeability and retention
FDA, U.S. Food and Drug Administration
GBCA, gadolinium-based contrast agent
HD, hydrodynamic diameter
ICP−MS, inductively coupled plasma mass spectrometry
MRI, magnetic resonance imaging
MWCO, molecular weight cut-off
NMR, nuclear magnetic resonance
PEG, polyethylene glycol
PET, positron emission tomography
ROI, region of interest
PTFE, polytetrafluoroethylene
SPECT, single-photon emission computed tomography
TEM, transmission electron microscopy
THF, tetrahydrofuran
uSPIO, ultra-small superparamagnetic iron oxide nanoparticle

■ REFERENCES

(1) Guo, B. J.; Yang, Z. L.; Zhang, L. J. Gadolinium Deposition in Brain: Current Scientific Evidence and Future Perspectives. *Front. Mol. Neurosci.* **2018**, *11*, 335.

(2) Johnson, N. J. J.; Oakden, W.; Stanisz, G. J.; Scott Prosser, R.; van Veggel, F. C. J. M. Size-Tunable, Ultrasmall NaGdF4 Nanoparticles: Insights into Their T1 MRI Contrast Enhancement. *Chem. Mater.* **2011**, *23*, 3714−3722.

(3) Gossuin, Y.; Gillis, P.; Hocq, A.; Vuong, Q. L.; Roch, A. Magnetic resonance relaxation properties of superparamagnetic particles. *Adv. Rev.* **2009**, *1*, 299−310.

(4) Rümenapp, C.; Gleich, B.; Haase, A. Magnetic Nanoparticles in Magnetic Resonance Imaging and Diagnostics. *Pharm. Res.* **2012**, *29*, 1165−1179.

(5) Laurent, S.; Forge, D.; Port, M.; Roch, A.; Robic, C.; Vander Elst, L.; Muller, R. N. Magnetic Iron Oxide Nanoparticles: Synthesis, Stabilization, Vectorization, Physicochemical Characterizations, and Biological Applications. *Chem. Rev.* **2008**, *108*, 2064−2110.

(6) Kwon, H. J.; Shin, K.; Soh, M.; Chang, H.; Kim, J.; Lee, J.; Ko, G.; Kim, B. H.; Kim, D.; Hyeon, T. Large-Scale Synthesis and Medical Applications of Uniform-Sized Metal Oxide Nanoparticles. *Adv. Mater.* **2018**, *30*, 1704290.

(7) Park, J.; An, K.; Hwang, Y.; Park, J.-G.; Noh, H.-J.; Kim, J.-Y.; Park, J.-H.; Hwang, N.-M.; Hyeon, T. Ultra-large-scale syntheses of monodisperse nanocrystals. *Nat. Mater.* **2004**, *3*, 891−895.

(8) Sperling, R. A.; Parak, W. J. Surface modification, functionalization and bioconjugation of colloidal inorganic nanoparticles. *Philos. Trans. R. Soc., A* **2010**, *368*, 1333−1383.

(9) Gupta, A. K.; Gupta, M. Synthesis and surface engineering of iron oxide nanoparticles for biomedical applications. *Biomaterials* **2005**, *26*, 3995−4021.
(10) Turcheniuk, K.; Tarasevych, A. V.; Kukhar, V. P.; Boukherroub, R.; Szunerits, S. Recent advances in surface chemistry strategies for the fabrication of functional iron oxide based magnetic nanoparticles. *Nanoscale* **2013**, *5*, 10729.
(11) Blanco, E.; Shen, H.; Ferrari, M. Principles of nanoparticle design for overcoming biological barriers to drug delivery. *Nat. Biotechnol.* **2015**, *33*, 941−951.
(12) Maeda, H.; Nakamura, H.; Fang, J. The EPR effect for macromolecular drug delivery to solid tumors: Improvement of tumor uptake, lowering of systematic toxicity, and distinct tumor imaging in vivo. *Adv. Drug Deliv. Rev.* **2013**, *65*, 71−79.
(13) Matsumura, Y.; Maeda, H. A new concept for macromolecular therapeutics in cancer chemotherapy: Mechanism of tumoritropic accumulation of proteins and the antitumor agent SMANCS. *Cancer Res.* **1986**, *46*, 6387−6392.
(14) Maeda, H.; Wu, J.; Sawa, T.; Matsumura, Y.; Hori, K. Tumor vascular permeability and the EPR effect in macromolecular therapeutics: a review. *J. Controlled Release* **2000**, *65*, 271−284.
(15) Du, Y.; Liu, X.; Liang, Q.; Liang, X.-J.; Tian, J. Optimization and Design of Magnetic Ferrite Nanoparticles with Uniform Tumor Distribution for Highly Sensitive MRI/MPI Performance and Improved Magnetic Hyperthermia Therapy. *Nano Lett.* **2019**, *19*, 3618−3626.
(16) Răcuciu, M.; Creanga, D. E.; Airinei, A. Citric-acid−coated magnetite nanoparticles for biological applications. *Eur. Phys. J. E* **2006**, *21*, 117−121.
(17) Mazur, M.; Barras, A.; Kuncser, V.; Galatanu, A.; Zaitzev, V.; Turcheniuk, K. V.; Woisel, P.; Lyskawa, J.; Laure, W.; Siriwardena, A.; Boukherroub, R.; Szunerits, S. Iron oxide magnetic nanoparticles with versatile surface functions based on dopamine anchors. *Nanoscale* **2013**, *5*, 2692−2702.
(18) Queffélec, C.; Petit, M.; Janvier, P.; Knight, D. A.; Bujoli, B. Surface Modification Using Phosphonic Acids and Esters. *Chem. Rev.* **2012**, *112*, 3777−3807.
(19) Huang, J.; Wang, L.; Zhong, X.; Li, Y.; Yang, L.; Mao, H. Facile non-hydrothermal synthesis of oligosaccharide coated sub-5 nm magnetic iron oxide nanoparticles with dual MRI contrast enhancement effects. *J. Mater. Chem. B* **2014**, *2*, 5344−5351.
(20) Sandiford, L.; Phinikaridou, A.; Protti, A.; Meszaros, L. K.; Cui, X.; Yan, Y.; Frodsham, G.; Williamson, P. A.; Gaddum, N.; Botnar, R. M.; Blower, P. J.; Green, M. A.; de Rosales, R. T. M. Bisphosphonate-Anchored PEGylation and Radiolabeling of Superparamagnetic Iron Oxide: Long-Circulating Nanoparticles for in Vivo Multimodal (T_1 MRI-SPECT) Imaging. *ACS Nano* **2013**, *7*, 500−512.
(21) Liu, Y.; Chen, T.; Wu, C.; Qiu, L.; Hu, R.; Li, J.; Cansiz, S.; Zhang, L.; Cui, C.; Zhu, G.; You, M.; Zhang, T.; Tan, W. Facile Surface Functionalization of Hydrophobic Magnetic Nanoparticles. *J. Am. Chem. Soc.* **2014**, *136*, 12552−12555.
(22) Ma, M.; Zhu, H.; Ling, J.; Gong, S.; Zhang, Y.; Xia, Y.; Tang, Z. Quasi-amorphous and Hierarchical Fe_2O_3 Supraparticles: Active T_1-Weighted Magnetic Resonance Imaging in Vivo and Renal Clearance. *ACS Nano* **2020**, *14*, 4036−4044.
(23) Xu, S.; Wang, J.; Wei, Y.; Zhao, H.; Tao, T.; Wang, H.; Wang, Z.; Du, J.; Wang, H.; Qian, J.; Ma, K.; Wang, J. *In Situ* One-Pot Synthesis of Fe_2O_3@BSA Core-Shell Nanoparticles as Enhanced T_1-Weighted Magnetic Resonance Imagine Contrast Agents. *ACS Appl. Mater. Interfaces* **2020**, *12*, 56701−56711.
(24) Ahangaran, F.; Hassanzadeh, A.; Nouri, S. Surface modification of Fe_3O_4@SiO_2 microsphere by silane coupling agent. *Int. Nano Lett.* **2013**, *3*, 23.
(25) Lee, H.; Dellatore, S. M.; Miller, W. M.; Messersmith, P. B. Mussel-inspired surface chemistry for multifunctional coatings. *Science* **2007**, *318*, 426−430.
(26) Schanze, K. S.; Lee, H.; Messersmith, P. B. Ten Years of Polydopamine: Current Status and Future Directions. *ACS Appl. Mater. Interfaces* **2018**, *10*, 7521−7522.
(27) Shultz, M. D.; Reveles, J. U.; Khanna, S. N.; Carpenter, E. E. Reactive nature of dopamine as a surface functionalization agent in iron oxide nanoparticles. *J. Am. Chem. Soc.* **2007**, *129*, 2482−2487.
(28) Lin, J. H. Bisphosphonates: A review of their pharmacokinetic properties. *Bone* **1996**, *18*, 75−85.
(29) Vllasaliu, D.; Fowler, R.; Stolnik, S. PEGylated nanomedicines: recent progress and remaining concerns. *Expet Opin. Drug Deliv.* **2014**, *11*, 139−154.
(30) Owen, J. The coordination chemistry of nanocrystal surfaces. *Science* **2015**, *347*, 615−616.
(31) Biju, V. Chemical modifications and bioconjugate reactions of nanomaterials for sensing, imaging, drug delivery and therapy. *Chem. Soc. Rev.* **2014**, *43*, 744−764.
(32) Kabachnik, M. I.; Medved, T. Y. New synthesis of aminophosphonic acids. *Dokl. Akad. Nauk SSSR* **1952**, *83*, 689−692.
(33) Fields, E. K. The Synthesis of Esters of Substituted Amino Phosphonic Acids. *J. Am. Chem. Soc.* **1952**, *74*, 1528−1531.
(34) Keglevich, G. The Kabachnik−Fields Reaction: Mechanism and Synthetic Use. *Molecules* **2012**, *17*, 12821−12835.
(35) Hapuarachchige, S.; Artemov, D. Click chemistry in the Development of Contrast Agents for Magnetic Resonance Imaging. *Top. Magn. Reson. Imag.* **2016**, *25*, 205−213.
(36) Kolb, H. C.; Finn, M. G.; Sharpless, K. B. Click Chemistry: Diverse Chemical Function from a Few Good Reactions. *Angew. Chem., Int. Ed.* **2001**, *40*, 2004−2021.
(37) Young, G. S.; Kimbrell, V.; Seethamraju, R.; Bubrick, E. J. Clinical 7T MRI for epilepsy care: Value, patient selection, technical issues, and outlook. *J. Neuroimaging* **2022**, *32*, 377.
(38) Shen, Y.; Goerner, F. L.; Snyder, C.; Morelli, J. N.; Hao, D.; Hu, D.; Li, X.; Runge, V. M. T1 Relaxivities of Gadolinium-Based Magnetic Resonance Contrast Agents in Human Whole Blood at 1.5, 3, and 7 T. *Invest. Radiol.* **2015**, *50*, 330−338.
(39) Robic, C.; Port, M.; Rousseaux, O.; Louguet, S.; Fretellier, N.; Catoen, S.; Factor, C.; Le Greneur, S.; Medina, C.; Bourrinet, P.; Raynal, I.; Idée, J.-M.; Corot, C. Physicochemical and Pharmacokinetic Profiles of Gadopiclenol: A New Macrocyclic Gadolinium Chelate With High T_1 Relaxivity. *Invest. Radiol.* **2019**, *54*, 475−484.
(40) Kanal, E. Gadolinium based contrast agents (GBCA): Safety overview after 3 decades of clinical experience. *Magn* **2016**, *34*, 1341−1345.
(41) Mazuel, F.; Espinosa, A.; Luciani, N.; Reffay, M.; Le Borgne, R.; Motte, L.; Desboeufs, K.; Michel, A.; Pellegrino, T.; Lalatonne, Y.; Wilhelm, C. Massive Intracellular Biodegradation of Iron Oxide Nanoparticles Evidenced Magnetically at Single-Endosome and Tissue Levels. *ACS Nano* **2016**, *10*, 7627−7638.

https://doi.org/10.1021/acsanm.2c01835
ACS Appl. Nano Mater. XXXX, XXX, XXX−XXX

2755

Development of USPIO-DM1-5D3-CF750: An image-guided targeted drug delivery system for prostate cancer therapy

Sudath Hapuarachchige[1,2], Ge Si[1,3], Catherine Foss[1], Cyril Barinka[4], and Dmitri Artemov[1,2]
[1]Department of Radiology and Radiological Science, The Johns Hopkins School of Medicine, Baltimore, MD, United States, [2]Department of Oncology, The Sidney Kimmel Comprehensive Cancer Center, Baltimore, MD, United States, [3]Department of Chemical and Biomolecular Engineering, The Johns Hopkins University, Baltimore, MD, United States, [4]Laboratory of Structural Biology, Institute of Biotechnology of the Czech Academy of Sciences, Vestec, Czech Republic

Synopsis

Prostate-specific membrane antigen (PSMA) is overexpressed in prostate cancers (PC) compared to normal tissues. Hence, PSMA can be used as a diagnostic biomarker and biological target to deliver drugs in PC therapy. In this study, we have conjugated ultra-small superparamagnetic iron oxide nanoparticles with mertansine (DM1), a chemotherapeutic drug, novel anti-PSMA 5D3 antibody, and NIR CF-750 fluorophore. This multimodality image-guided drug delivery system was evaluated in PC mouse models using in vivo fluorescent imaging and MRI at 9.4T. Promising results encourage further development of targeted image-guided drug delivery platforms for PC therapy.

Purpose

To develop an image-guided and targeted drug delivery system for utilizing ultra-small super paramagnetic iron oxide (USPIO) nanoparticles, 5D3 anti-PSMA monoclonal antibody, mertansine (DM1) anti-tubulin drug, and near-infrared fluorophore for prostate cancer therapy.

Methods

Prostate cancer (PC) is the most common cancer in men. It is associated with the second highest cancer related mortality.[1] PC eventually becomes castrate-resistant prostate cancer (CRPC) and progresses rapidly to metastatic form (mCRPC).[2] In these mCRPC stages, drugs, such as docetaxel and cabazitaxel lack efficacy and can produce significant toxic effects in healthy tissues and organs. Prostate-specific membrane antigen (PSMA) is overexpressed in practically all malignant PC compared to non-prostatic and non-malignant tissues.[3] Its expression is also related to cancer aggressiveness and androgen blockage and deprivation is further enhancing PSMA levels. Hence, PSMA can be used as a biomarker to deliver drugs to PSMA(+) PC. PSMA-specific antibodies, peptides and small molecules are widely used as bioligands to target PSMA for imaging and therapy.[4] Novel anti-PSMA monoclonal antibody (mAb), 5D3, has been successfully used for imaging and drug delivery in PSMA(+) PC.[5-6] This antibody has higher PSMA binding affinity than other existing PSMA-targeting antibodies.[7] Ultra-small superparamagnetic iron oxide (USPIO) nanoparticles are biocompatible, can be detected with high sensitivity by MRI, and have high loading capacity for cargo molecules. Therefore, USPIO platforms are highly relevant for development of MRI-guided drug delivery. Specific delivery of SPIO nanoparticles to target tumors can be achieved by decorating their surface with target-specific mAb.[8]

In this report we have developed a novel USPIO-5D3 targeted MRI-detectable platform to deliver chemotherapeutics to PSMA(+) PC. 5D3 mAb targeted USPIO nanoparticles were also conjugated with mertansine (DM1), a highly-potent anti-tubulin drug, to obtain USPIO-DM1-5D3 drug delivery system. This complex was further conjugated with near-infrared (NIR) fluorophore for optical tracking of the delivery. This final multimodality theranostic image-guided drug delivery system, USPIO-DM1-5D3-CF750 (shown in Figure 1A) combines both therapeutic and image-guided diagnostic capabilities. Biodistribution and tumor uptake of USPIO-DM1-5D3-CF750 were studied in PSMA(±) tumor mouse models. The PSMA(+) and PSMA(-) dual tumor mouse models were prepared by inoculation of PC3-Flu and PC3-PIP cells in the right and left flank of mice, respectively. Mice were injected with USPIO-DM1-5D3-CF750 nano-theranostics (Total-weight dose: 5 mg/kg) i.v. and imaged after 1 h and 24 h using Xenogen in vivo live animal optical imaging system. The results show high tumor uptake of nano-theranostics in PSMA(+) PC3-PIP tumor (Figure 1B). We also observed high liver uptake of the nano-theranostics and renal excretion of CF-750. After 24 h, mice were euthanized and tumors and vital organs, brain, heart, lungs, liver, kidneys, spleen, and intestine were extracted and imaged ex vivo using Xenogen. MRI images were taken after systemic i.v. administration of USPIO-DM1-5D3-CF750 (Total-weight dose: 10 mg/kg) in dual tumor mouse models (Figure 2) using a 9.4T Bruker small animal MRI system. We observed a significant change in T1 contrast in tumors compared to the pre-scan; however, the T1 contrast difference between PSMA(+) and PSMA(-) tumors was not significant (Figure 2A). T2-weighted images showed considerably higher contrast of USPIO-DM1-5D3-CF750 uptake in PSMA(+) tumors compared to PSMA(-) tumor (Figure 2B). We are currently determining MR relaxation properties of the nano-theranostics and evaluating significance of the tumor uptake. We are also optimizing the conjugation chemistry and evaluating USPIO with different surface functional groups. This study fosters a strong foundation to develop a highly effective image-guided drug delivery system, using biocompatible, high-capacity USPIO nanoparticles, high PSMA affinity 5D3 mAb, and highly potent mertansine (DM1) chemotherapeutics to treat PSMA-overexpressing PC.

Acknowledgements

This study was supported by the DOD (W81XWH-20-1-0429) grant and Emerson Collective Cancer Research Fund (128821-2018).

References

1. Siegel, R. L.; Miller, K. D.; Jemal, A. Cancer Statistics, 2020. CA Cancer J Clin. 2020; 70: 7-30.

2. Cho, S.; Zammarchi, F.; Williams, D. G. et al. Antitumor Activity of MEDI3726 (ADCT-401), a Pyrrolobenzodiazepine Antibody-Drug Conjugate Targeting PSMA, in Preclinical Models of Prostate Cancer. Mol Cancer Ther. 2018; 17: 2176-2186.

3. Israeli, R. S.; Powell, C. T.; Corr, J. G. et al. Expression of the Prostate-Specific Membrane Antigen. Cancer Res. 1994; 54: 1807-1811.

4. Boinapally, S.; Ahn, H.; Cheng, B. et al. A Prostate-Specific Membrane Antigen (PSMA)-Targeted Prodrug with a Favorable in vivo Toxicity Profile. Sci. Rep. 2021; 11: Article No. 7114.

5. Hapuarachchige, S. Huang, C. T.; Donnelly, M. C. et al. Cellular Delivery of Bioorthogonal Pretargeting Therapeutics in PSMA-Positive Prostate Cancer. Mol Pharm 2020; 17: 98-108.

6. Colin, T. H. Guo, X.; Barinka, C. et al. Development of 5D3-DM1: A Novel Anti-Prostate-Specific Membrane Antigen Antibody-Drug Conjugate for PSMA-Positive Prostate Cancer Therapy. Mol. Pharmaceutics 2020; 17: 3392–3402.

7. Novakova, Z.; Foss, C. A.; Copeland, B. T. et al. Novel Monoclonal Antibodies Recognizing Human Prostate-Specific Membrane Antigen (PSMA) as Research and Theranostic Tools. Prostate 2017; 77: 749-764.

8. Julien, D. C. Behnke, S.; Wang, G. et al. Utilization of Monoclonal Antibody-Targeted Nanomaterials in the Treatment of Cancer. MAbs. 2011; 3: 467–478.

Figures

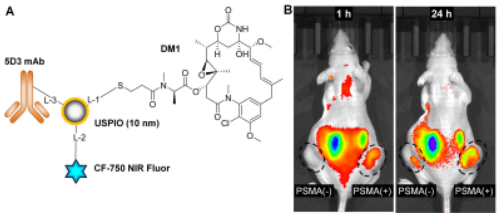

Figure 1. Synthesis and NIR optical images of USPIO-DM1-5D3-CF750 in mouse PC models. **(A).** The structure of the USPIO-DM1-5D3-CF750. **(B).** *In vivo* Xenogen NIR optical images of a mouse treated with USPIO-DM1-5D3-CF750.

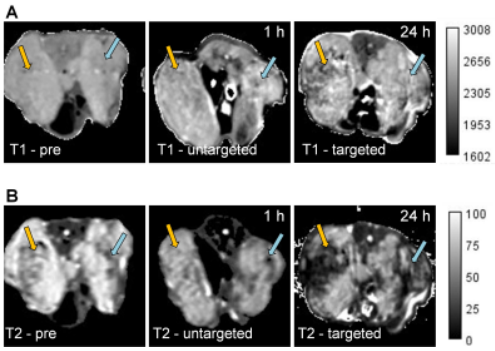

Figure 2. T1 **(A)** and T2 **(B)** images of PSMA(+) tumors (yellow arrow) and PSMA(-) tumors (blue arrows) before treatment, treated with untargeted USPIO (without 5D3 conjugation), and treated with USPIO-DM1-5D3-CF750 after 1h and 24 h.

Optical- and MRI-detectable USPIO-5D3-DM1 nano-constructs for prostate cancer therapy

Sudath Hapuarachchige[1,2], Ge Si[1,3], Cyril Barinka[4], Dmitri Artemov[1,2]*

Introduction: Prostate cancer (PC) has the second highest cancer related mortality in men.[1] Primary PC eventually becomes castrate resistant (CRPC) stage and progresses rapidly to lethal metastatic form (mCRPC).[2] In mCRPC stage, common chemotherapeutics such as docetaxel and cabazitaxel show an insufficient therapeutic efficacy. They also exhibit significant non-specific toxicities for vital organs and side effects. Prostate-specific membrane antigen (PSMA) are cell surface receptors expressed in prostate tissues; they are overexpressed in almost all PCs compared to non-prostatic tissues.[3] This expression level is also corelated with cancer aggressiveness, androgen blockage and deprivation. Therefore, PSMA is widely used as a natural biomarker for PC targeted drug delivery. PSMA-specific biomacromolecules such as anti-PSMA antibodies and peptides, and target-specific small molecules are currently used as bioligands for PSMA.[4]
In this study, an original antibody-targeted ultrasmall iron oxide (USPIO) nanoparticle-based drug delivery system was developed for image-guided drug delivery in PC. A recently developed anti-PSMA monoclonal antibody (mAb), 5D3, was used as the bioligand.[5-6] 5D3 mAb has improved PSMA binding affinity and internalization characteristics compared to other existing anti-PSMA mAbs.[7] USPIO have high loading capacity and biocompatibility, as a drug delivery platform. They can be detected *in vivo* by magnetic resonance imaging (MRI) as well.

Methods: First, 5D3 mAb was conjugated with USPIO nanoparticles and loaded with mertansine (DM1), an anti-tubulin agent, as the chemotherapeutic drug to obtain USPIO-5D3-DM1. The nano-construct was further labeled with near-infrared (NIR) fluorophore, CF-750 for optical imaging and tracking the delivery. The final USPIO-5D3-DM1-CF750 (Figure 1A) nano-construct has both therapeutic and diagnostic capabilities. The biodistribution and tumor uptake of USPIO-5D3-DM1-CF750 were evaluated in PSMA(±) xenograft mouse models. Bilateral tumor mouse models were prepared by the inoculation of PSMA(+) PC3-PIP and PSMA(-) PC3-Flu cells. Mice were administered with USPIO-5D3-DM1-CF750 nano-constructs (5.0 mg/kg in Saline, i.v.) and imaged using Xenogen *in vivo* live animal optical imaging system.

Results: The results show high tumor uptake of nano-construct in PSMA(+) PC3-PIP tumor (Figure 1B). After 24 h, mice were euthanized and tumors and vital organs, brain, heart, lungs, liver, kidneys, spleen, and intestine were extracted and imaged *ex vivo* using Xenogen (Figure 1C). High uptake of the probe was confirmed in PSMA(+) tumor, as well as in the liver and kidneys. MR images were taken after systemic administration of USPIO-5D3-DM1-CF750 (10.0 mg/kg, i.v.) in bilateral tumor mouse models using a 9.4T Bruker Biospin MRI system. A significant change in T1 contrast was observed in tumors compared to the pre-scan (Figure 1D). T2-weighted images exhibited considerably higher contrast of USPIO-5D3-DM1-CF750 uptake in PSMA(+)than in PSMA(-) tumors. Currently, MR relaxation properties of the nano-constructs and tumor uptake of drugs are being investigated.

Conclusions: This study establishes a strong foundation for the development of highly effective image-guided drug delivery system, using biocompatible, high-capacity USPIO drug carrier nanoparticles, high PSMA affinity 5D3 targeting mAb, and highly potent DM1 chemotherapeutics to treat PSMA-overexpressing PC.

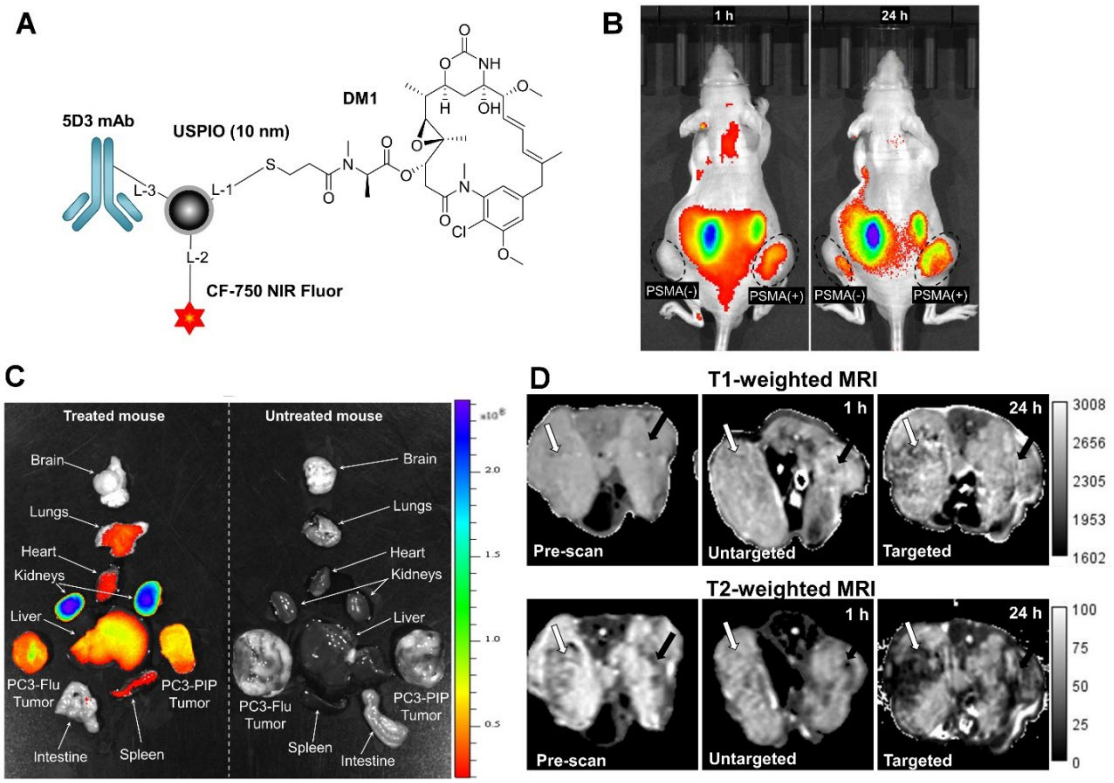

Figure 1. Development and evaluation of USPIO-5D3-DM1-CF750. **(A)** The structure of USPIO-5D3-DM1-CF750. (B) *In vivo* Xenogen NIR optical images of a mouse treated with USPIO-5D3-DM1-CF750. **(C)** *Ex vivo* images of vital organs and tumors showing biodistribution and tumor uptake. **(D)** T1-weighted and T2-weighted images of PSMA(+) tumors (white arrows) and PSMA(-) tumors (black arrows) before treatment and at 1h and 24 h after treatment with USPIO-5D3-DM1-CF750 carriers or control untargeted USPIO without 5D3 conjugation.

References:

1. Siegel, R. L.; Miller, K. D.; Jemal, A. Cancer Statistics, 2020. CA Cancer J Clin. 2020; 70: 7-30.
2. Cho, S.; Zammarchi, F.; Williams, D. G. et al. Antitumor Activity of MEDI3726 (ADCT-401), a Pyrrolobenzodiazepine Antibody-Drug Conjugate Targeting PSMA, in Preclinical Models of Prostate Cancer. Mol Cancer Ther. 2018; 17: 2176-2186.
3. Israeli, R. S.; Powell, C. T.; Corr, J. G. et al. Expression of the Prostate-Specific Membrane Antigen. Cancer Res. 1994; 54: 1807-1811.
4. Boinapally, S.; Ahn, H.; Cheng, B. et al. A Prostate-Specific Membrane Antigen (PSMA)-Targeted Prodrug with a Favorable in vivo Toxicity Profile. Sci. Rep. 2021; 11: Article No. 7114.
5. Hapuarachchige, S. Huang, C. T.; Donnelly, M. C. et al. Cellular Delivery of Bioorthogonal Pretargeting Therapeutics in PSMA-Positive Prostate Cancer. Mol Pharm 2020; 17: 98-108.
6. Colin, T. H. Guo, X.; Barinka, C. et al. Development of 5D3-DM1: A Novel Anti-Prostate-Specific Membrane Antigen Antibody-Drug Conjugate for PSMA-Positive Prostate Cancer Therapy. Mol. Pharmaceutics 2020; 17: 3392–3402.
7. Novakova, Z.; Foss, C. A.; Copeland, B. T. et al. Novel Monoclonal Antibodies Recognizing Human Prostate-Specific Membrane Antigen (PSMA) as Research and Theranostic Tools. Prostate 2017; 77: 749-764.